

Stellar activity by spot transit modeling

Adriana Valio¹

¹ Centro de Rádio Astronomia e Astrofísica Mackenzie (CRAAM), Universidade Presbiteriana Mackenzie
e-mail: avalio@craam.mackenzie.br

Abstract. Currently, of the 3780 planets detected, 2812 eclipses its host star, 2303 of which were discovered by the Kepler satellite. During a transit of a planet in front of its host star, it may occult stellar features such as spots or faculae. This will cause small variations in the star light curve. Detailed analysis of these variations provides a wealth of information about starspot properties such as size, position, temperature (i.e. intensity), and magnetic field. If the same spot is detected in a later transit, it is possible to estimate the stellar rotation period, as Galileo did for the Sun four centuries ago. Moreover, the differential rotation of the star can also be inferred. This study is performed using a method that simulates the passage of a planet (dark disk) in front of a star with multiple spots of different sizes, intensities, and positions on its surface. The ECLIPSE algorithm developed is available in Python. We present the results of the spots properties obtained from the analyses of the light curves of CoRoT-2, Kepler-17, Kepler- 63 and Kepler-71.

Resumo. Atualmente, dos 3780 planetas detectados, 2812 eclipsam sua estrela hospedeira, dos quais 2.303 foram descobertos pelo satélite Kepler. Durante o trânsito de um planeta em frente à sua estrela, fenômenos fotosféricos como manchas ou faculas podem ser ocultados, causando pequenas variações na curva da luz da estrela. A análise detalhada destas variações fornece uma riqueza de informações sobre as propriedades de manchas, tais como tamanho, posição, temperatura (isto é intensidade) e campo magnético. Se a mesma mancha for detectada em um trânsito posterior, é possível estimar o período de rotação estelar, assim como Galileu fez para o Sol, mais de quatro séculos atrás. Além disso, a rotação diferencial da estrela também pode ser inferida. Este estudo é realizado usando um método que simula a passagem de um planeta (disco escuro) em frente a uma estrela com múltiplas manchas de diferentes tamanhos, intensidades e posições em sua superfície. O algoritmo ECLIPSE desenvolvido em Python está disponível. Apresentamos os resultados das propriedades das manchas obtidos a partir das análises das curvas de luz das estrelas CoRoT-2, Kepler-17, Kepler-63 e Kepler-71.

Keywords. Stars: starspots – Stars: rotation – Planetary Systems

1. Introduction

Sunspots were the first indications of solar activity, being reported since the ancient Chinese. Since Galileo, over four centuries ago, sunspots have been routinely monitored. Very likely, all cool stars with a convective envelope like the Sun also have spots on their surfaces. Unfortunately, current telescopes do not have the spatial resolution to detect spots similar to sunspots. Nevertheless, a few techniques were developed to study starspots.

Doppler imaging of fast rotating, young stars has shown that these have many large spots on their surface (Strassmeier, 2009). These same spots also cause modulation of the total brightness of the star as the spots rotate in and out of view (Lanza et al., 2009). This modulation can reach up to 10% peak-to-peak. In the case of the Sun, this modulation is seldom larger than 0.1%. Finally, the method developed by Silva (2003), uses planetary transits as a probe to study the characteristics of spots.

Presently, almost 4000 planets have been discovered (www.exoplanet.eu/catalog/), most of them (73%) by planetary transits, that is, small periodic decreases detected in the light curve as the planet eclipses the host star. In the case of a solar type star, the decrease in flux is 1% for a Jupiter size planet, whereas for a terrestrial one of Earth size, the decrease in flux is about 0.01%.

Here we analyze the light curve of active stars with transiting planets to search for spot signatures. The stars studied and their planets are listed in Table 1.

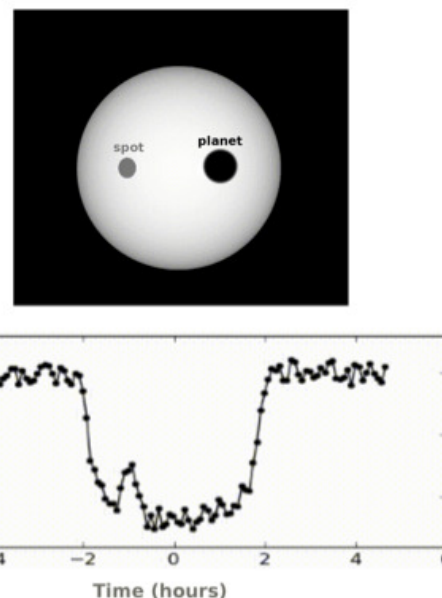


FIGURE 1. Top: Model of star with limb darkening and one spot (left), also shown is the planet as it transits in front of the stellar disk. Bottom: Light curve (with noise) of simulated transit with the signal of the spot evident at -1.5h.

Table 1. Stellar and planetary parameters.

Star	CoRoT-2 ^a	Kepler-17 ^b	Kepler-63 ^c	Kepler-71 ^d
Spectral type	G7 V	G2 V	G8 V	G7 V
Mass (M_{sun})	0.97	1.16	0.98	0.997
Radius (R_{sun})	0.902	1.01	0.90	0.887
T_{eff} (K)	5625	5781	5576	5540
Planet				
Mass (M_{Jup})	3.31	2.45	–	–
Radius (R_{Jup})	0.172	0.138	0.066	0.136
Orbital period (d)	1.743	1.49	9.434	3.905
Semi-major (R_{star})	6.7	5.73	19.55	12.186

^a Silva-Valio & Lanza (2011)

^b Valio et al. (2017)

^c Netto & Valio (2017)

^d Zaleski et al. (2019)

2. Model and Spots characteristics

Silva (2003) was the first to develop a model to study the signatures of starspots on the surface of other stars. As the planet eclipses the star, it may occult a dark spot, this will cause a slight increase in brightness during the transit (see Figure 1). By modeling these “bumps”, it is possible to infer the spots physical characteristics as will be detailed later.

The star is modeled as a circular bright disk with limb darkening (linear or quadratic given by Eq. 1), whereas the planet is a dark disk with a radius that is a fraction of the stellar radius, in circular orbit (null eccentricity) with a semi-major axis also measured in units of planetary radius, and inclination angle. The orbital period is an input to the model.

Furthermore, the spots are modeled by three parameters: its intensity, that depends on the temperature, with respect to the maximum stellar intensity at disk center, I_c ; its size in units of planetary radius; and position, latitude and longitude on the stellar hemisphere. The foreshortening effect of the spot projection is taken into account when it is close to the limb.

An example of the spot modeling is shown in Figure 2. First, a spotless star model is built, by fitting five parameters: the planet radius, the orbital semi-major axis, a , inclination angle, i , and the two limb darkening coefficients, u_1 and u_2 given by Eq. 1.

$$\frac{I(\mu)}{I_c} = 1 - u_1(1 - \mu) - u_2(1 - \mu)^2 \quad (1)$$

where I_c is the stellar central intensity.

The result is the U-shaped transit, shown by the blue dashed line in the top panel of Figure 2. Once the spotless transit model is satisfactory, this is subtracted from the observed lightcurve, yielding the residuals. The spot signatures are much more clearly seen in the residuals (see bottom panel of Figure 2). These “bumps”, assumed to be due to starspots, are then fit by three parameters each: intensity, radius, and longitude. Since the rotation period of the star (order of days) is much longer than the transit duration (order of hours), it is reasonable to assume that the spot position (longitude) does not vary during the transit. Hence, the longitude of the spot, long_s is related to the observed time of the “bump”, t_s .

$$\text{long}_s = \arcsin \left[\frac{a \cos \left(90^\circ - \frac{360^\circ t_s}{24 P_{orb}} \right)}{\cos(\text{lat})} \right] \quad (2)$$

where P_{orb} is the orbital period, a the semi-major axis, and $\text{lat} = \arcsin[a/(R_{star}\cos(i))]$ is the latitude of the transit, if the planet

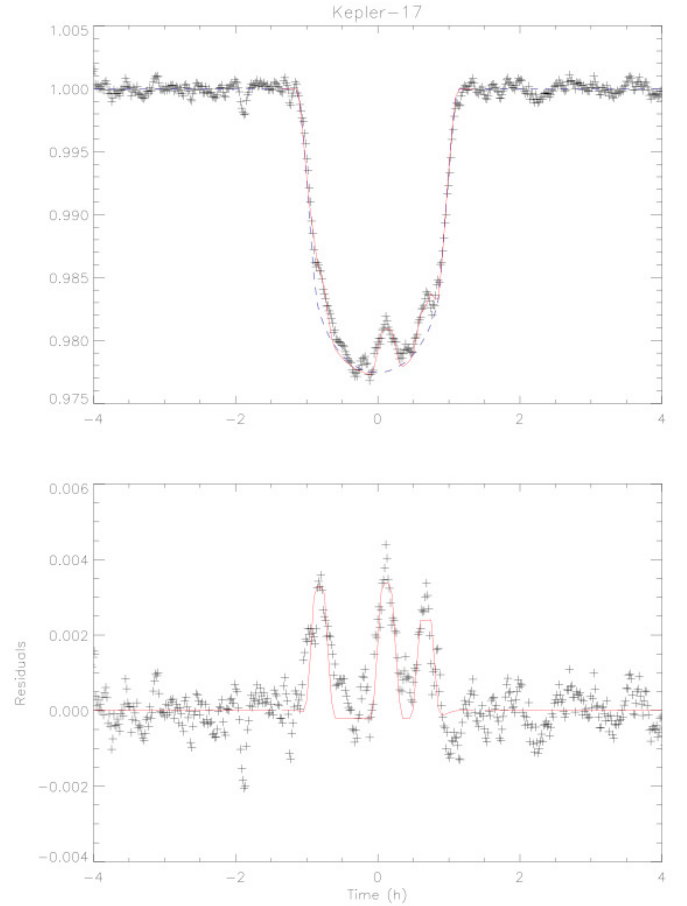


FIGURE 2. Top: Light curve of a Kepler-17b transit (black crosses). The model of the star without any spots is depicted as the blue dashed line, whereas the model with three spots is shown in red. Bottom: The residuals of the light curve after subtraction of the spotless model (dashed blue line in top panel). The red curve depicts the fit of the three spots.

orbit is assumed to be coplanar with the stellar equator. This projected transit latitude is listed in the first row of Table 3. The negative sign is arbitrarily assumed and represents a Southern hemisphere transit.

Table 2. Spots physical characteristics

Star	CoRoT-2	Kepler-17	Kepler-63	Kepler-71	Sun
Radius (Mm)	55 ± 19	80 ± 50	26 ± 5	41 ± 9	12 ± 10
Area (%)	13 ± 5	11 ± 1.5	4.9 ± 2.5	2.5 ± 0.9	< 1
T_s (K)	4600 ± 700	5100 ± 500	4700 ± 300	4100 ± 800	4800 ± 400

Table 3. Stellar rotation and differential rotation parameters.

Star	CoRoT-2	Kepler-17	Kepler-71	Sun
Latitude ($^\circ$)	-14.6	-4.6	-5.4	
P_{ave} (d)	4.54	12.28	6.35	27.6
$P(lat)$ (d)	4.48	11.4	6.08	24.7
$\Delta\Omega$ (rd/d)	0.042	0.077	0.005	0.050
$\Delta\Omega/\Omega$ (%)	3.0	15.0	2	22.1

Assuming blackbody emission for the spot, T_s , as well as the surrounding photosphere, the temperature of the spot can be inferred:

$$T_s = \frac{K_b}{h\nu \ln(f_i(e^{h\nu/KT_{eff}} - 1) + 1)} \quad (3)$$

where K_b and h are the Boltzmann and Planck constants, respectively, T_{eff} is the photospheric, ν is the observation frequency, and f_i is the ratio of spot intensity with respect to the central stellar intensity I_c .

The results of the spot modelling for the stars listed in Table 1 are given in Table 2. For comparison, the last column lists the characteristics of sunspots. The average radius of spots, in units of $10^6 m$, is listed in the first row, whereas the second row shows the area of the stellar surface covered by spots. The last row brings the average temperature of spots given by Eq. 3.

As can be seen from the results, the spots on other stars are larger than those of the Sun. This is not surprising since these other stars are significantly more active than our star. Besides, these sizes are probably related to active regions, rather than individual spots. Since the spots are larger, so is the relative surface area covered by spots. As for the temperature, stars with higher photospheric temperatures have warmer spots than the cooler stars.

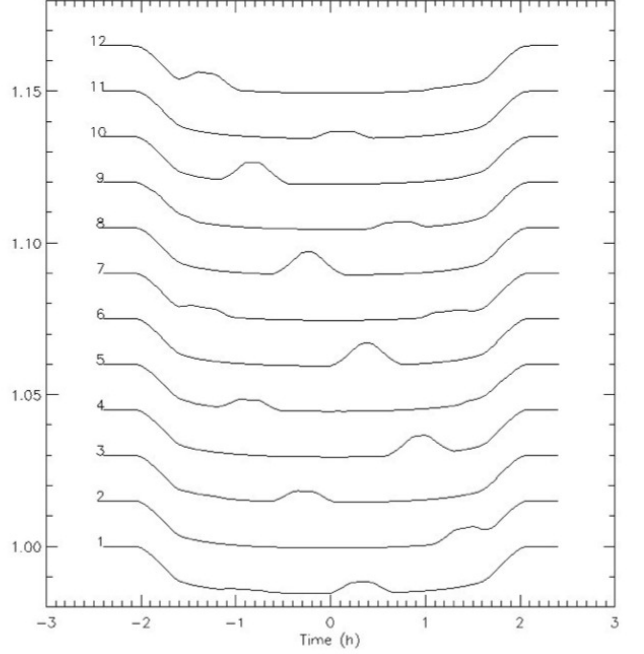
3. Stellar rotation and differential rotation

Silva-Valio (2008) describes how to measure the rotation period of a star by tracking a spot on more than one transit. If the same spot is detected in a subsequent transit, as shown in Figure 3, the rotation period of the star can be measured. However, this will be the period at the projected latitude of the transit.

For that, a coordinate system transformation is needed from one centered on Earth, to a coordinate system that rotates with the star of rotation period P_{star} . This period is estimated by calculating the autocorrelation of the spot flux deficit for each transit, for a given P_{star} . By varying P_{star} and determining the width of the autocorrelation function, the rotation period of the star will be that of the thinnest autocorrelation function (Valio, 2013).

The stellar rotation periods estimated this way are listed in the third row of Table 3. Again the last column lists the solar values for comparison. The case of Kepler-63 star is more complicated because the planet is in an almost polar orbit, thus the assumption of coplanar orbit cannot be made.

This method has been compared with the Maximum Entropy Method applied to the out-of-transit light curve for the CoRoT-2 star (Silva-Valio & Lanza, 2011).


FIGURE 3. Twelve simulated transits of a star with 4 spots.

To estimate the differential rotation of the star, we assume a solar like rotation profile of the type:

$$\Omega = A - B \sin^2(lat) \quad (4)$$

where Ω is the angular rotation at a given latitude, lat , and B represents the shear due to differential rotation in rd/d. To determine the A and B constants, we need another equation. For this we consider the average period of the star, P_{ave} . This average period is obtained by calculating the Lomb-Scargle periodogram from the out-of-transit light curve. Thus, the second equation is:

$$\bar{\Omega} = \frac{1}{(\alpha_2 - \alpha_1)} \int_{\alpha_1}^{\alpha_2} (A - B \sin^2 \alpha) d\alpha \quad (5)$$

where $\bar{\Omega} = 2\pi/P_{ave}$, and α_1 and α_2 are the minimum and maximum latitudes where spots appear, respectively. The average period is listed in the second row of Table 3. Now, combining Eqs. 4 and 5, the constants A and B can be determined. To simplify, we assume $\alpha_1 = 0$ and $\alpha_2 = 90^\circ$. The resulting shear or differential rotation, $\Delta\Omega = B$, and the relative differential rotation, $\Delta\Omega/\bar{\Omega}$, are given in the two last rows of the table.

4. Magnetic field and magnetic cycles

Estrela & Valio (2017) has analyzed the spots detected in the lightcurves of the Kepler-17 and Kepler-63 stars. Almost 1000 spots were fit in the case of Kepler-17, whereas for Kepler-63 this number approached 300. The flux deficit due to spots for Kepler-17 is plotted in Figure 4. From this curve a period of 410

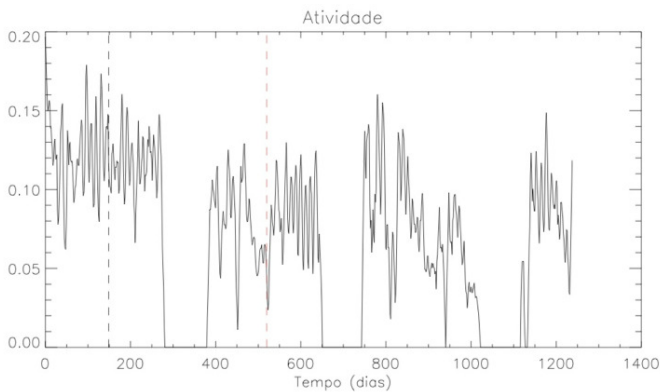


FIGURE 4. Flux deficit caused by the spots seen in Kepler-17 in time during the 4 years observation. The dashed blue line shows a period of maximum activity, or many spots on the surface of the star, whereas the red dashed line depict a period of minimum activity.

days, or 1.13 yr were estimated from the Lomb-Scargle periodogram. A similar analysis was applied to Kepler-63, yielding a period of 460 days, or 1.3 yr. These periodicities in the number of spots on the surface of the stars were assumed to be due to a magnetic cycle.

Due to the limitation of the 4 year observing of the Kepler satellite, the magnetic cycle may be longer. Nevertheless these periods may be similar to the quasi biannual cycles observed for the Sun.

One last estimate that can be made is the magnetic field intensity of these starspots. Dicke (1970) suggested that the temperature of sunspots decreased with the increase in intensity of the spot magnetic field in a quadratic way:

$$\frac{T_s}{T_{\text{eff}}} = c_1 - c_2 B^2 \quad (6)$$

This can be seen in Figure 5, for the study of over 30,000 sunspots studied for the solar activity cycle 23 (Spaggiari & Valio, 2014). By inverting this equation, the magnetic field of starspots can be inferred:

$$B = \sqrt{\frac{1}{c_2} \left(c_1 - \frac{T_s}{T_{\text{eff}}} \right)} \quad (7)$$

The ratio T_s/T_{eff} is determined from the intensity fit of the spot (Eq. 3). By applying Equation 7 to the data obtained for CoRoT-2 and Kepler-17, we obtained magnetic field intensities of (1700 ± 700) G and (1400 ± 500) G, respectively. For comparison, the average value of the sunspots observed during cycle 23 is (700 ± 350) G. This is no surprise, since both CoRoT-2 and Kepler-17 stars are much younger than our Sun, with ages of 0.13 – 0.5 and 1.78 Gyr, respectively.

5. Summary and conclusions

Younger stars are very active with many spots on their surfaces. When a planet transits in front of its host star, it may occult one such spot. This signature will be visible in the transit lightcurve as a “bump”, that can be enhanced in the residuals of the light curve. A model was developed by Silva (2003) to determine the physical characteristics of these spots, such as size, temperature and even magnetic field. This spot model has been applied so far to the stars CoRoT-2, Kepler-17, Kepler-63, and Kepler-71.

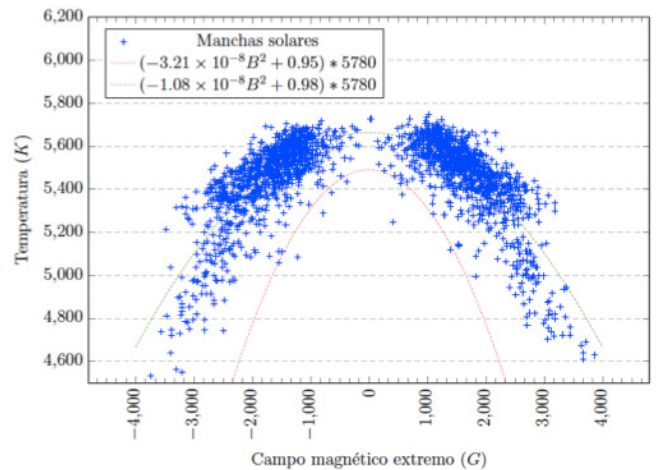


FIGURE 5. Temperature and magnetic field relation for sunspots observed for cycle 23 (blue dots). The green line represent a quadratic fit to these points, whereas the red line is a previous fit by Dicke (1970).

When the same spot is observed in multiple transits, the stellar rotation period at the projected latitude may be estimated (Silva-Valio, 2008). Moreover, the differential rotation, or shear, can be calculated by considering also the average rotation period estimated from the out-of-transit data (Silva-Valio et al., 2010; Silva-Valio & Lanza, 2011; Netto & Valio, 2017; Valio et al., 2017).

The magnetic field intensity of spots can be inferred from their solar counterparts, using the same quadratic relation between temperature (or intensity) and magnetic field. This was done for the spots of CoRoT-2 and Kepler-17 yielding spots with stronger magnetic field intensities.

Counting the flux deficit caused by the presence of starspots, which is a proxy for the number of spots on the surface of the star, throughout the years of observation of the Kepler satellite, can give an idea of short magnetic activity cycles. This study was done for Kepler-17 and Kepler-63 resulting in magnetic cycle periodicities slightly larger than a year (Estrela & Valio, 2017).

Acknowledgements. We thank the research funding agency FAPESP (São Paulo Research Foundation) for partial financial support.

References

- Dicke, R.H. 1970, *ApJ*, 159, 25.
- Estrela, R. & Valio, A. 2017, *ApJ*, 831, 57
- Lanza, A.F. et al. 2009, *A&A*, 493, 193
- Netto, Y. & Valio, A. 2017, In: *Living Around Active Stars, Proceedings of the International Astronomical Union, IAU Symposium, 328, 107-109*
- Silva, A. 2003, *ApJ (Letters)*, 585, L147
- Silva-Valio, A. 2008, *ApJ (Letters)*, 683, L179
- Silva-Valio, A., Lanza, A. F., Alonso, R., Barge, P. 2010, *A&A*, 510, 25
- Silva-Valio, A. & Lanza, A.F. 2011, *A&A*, 529, 36
- Spaggiari, E. & Valio, A. 2014. In: *Magnetic Fields throughout Stellar Evolution, Proceedings of the International Astronomical Union, IAU Symposium, 302, 220-221*
- Strassmeier, K. G. 2009, *A&A*, 17, 251
- Valio, A. 2013, *PASP*, 472, 239
- Valio, A., Estrela, R., Netto, Y., Bravo, J. P., de Medeiros, J.R. 2017, *ApJ*, 835, 294
- Zaleski, S.M., Valio, A., Marsden, S.C., & Carter, B.D. 2019, *MNRAS* (accepted)